Valence and conduction band offsets of ß-Ga2O3/AlN heterojunction

Valence and conduction band offsets of β–Ga_2O_3/AlN heterojunction

Haiding Sun, C. G. Torres Castanedo, Kaikai Liu, Kuang-Hui Li, Wenzhe Guo, Ronghui Lin, Xinwei Liu, Jingtao Li, and Xiaohang Li

Citation: Appl. Phys. Lett. **111**, 162105 (2017); doi: 10.1063/1.5003930
View online: http://dx.doi.org/10.1063/1.5003930
View Table of Contents: http://aip.scitation.org/toc/apl/111/16
Published by the American Institute of Physics

Valence and conduction band offsets of β-Ga_2O_3/AlN heterojunction

Haiding Sun, C. G. Torres Castanedo, Kaikai Liu, Kuang-Hui Li, Wenzhe Guo, Ronghui Lin, Xinwei Liu, Jingtao Li, and Xiaohang Li
King Abdullah University of Science and Technology (KAUST), Advanced Semiconductor Laboratory, Thuwal 23955-6900, Saudi Arabia

(Received 8 September 2017; accepted 5 October 2017; published online 16 October 2017)

Both β-Ga_2O_3 and wurtzite AlN have wide bandgaps of 4.5–4.9 and 6.1 eV, respectively. We calculated the in-plane lattice mismatch between the (−201) plane of β-Ga_2O_3 and the (0002) plane of AlN, which was found to be 2.4%. This is the smallest mismatch between β-Ga_2O_3 and binary III-nitrides which is beneficial for the formation of a high quality β-Ga_2O_3/AlN heterojunction. However, the valence and conduction band offsets (VBO and CBO) at the β-Ga_2O_3/AlN heterojunction have not yet been identified. In this study, a very thin (less than 2 nm) β-Ga_2O_3 layer was deposited on an AlN/sapphire template to form the heterojunction by pulsed laser deposition. High-resolution X-ray photoelectron spectroscopy revealed the core-level (CL) binding energies of Ga 3d and Al 2p with respect to the valence band maximum in individual β-Ga_2O_3 and AlN layers, respectively. The separation between Ga 3d and Al 2p CLs at the β-Ga_2O_3/AlN interface was also measured. Eventually, the VBO was found to be -0.55 ± 0.05 eV. Consequently, a staggered-gap (type II) heterojunction with a CBO of -1.75 ± 0.05 eV was determined. The identification of the band alignment of the β-Ga_2O_3/AlN heterojunction could facilitate the design of optical and electronic devices based on these and related alloys. *Published by AIP Publishing.*
https://doi.org/10.1063/1.5003930

In the past few decades, conventional group-III-nitrides (GaN, AlN, and InN) and their alloys have been widely used for optoelectronic and power devices because of their tunable bandgaps and chemical stability.[1–4] The β-polytype of Ga_2O_3 has an extremely high breakdown field of ∼8 MV/cm, which is higher than that of SiC (3 MV/cm) and GaN (3.8 MV/cm), and thus, it has become attractive for power electronics.[5,6] Recently, over 1 kV of reverse breakdown voltage in a vertical diode was achieved by using β-Ga_2O_3.[7] In addition, because of its large intrinsic bandgap of 4.5–4.9 eV, it is suitable for solar-blind deep ultraviolet detection.[8,9] Due to its chemical and thermal stability, it can be utilized in extreme environment electronics, such as toxic gas sensors.[10] Most importantly, β-Ga_2O_3 can be obtained in the bulk form from melt sources. The availability of large-size and high-quality single-crystal wafers that can be fabricated at low cost from melt-grown bulk crystals is a remarkable advantage over other conventional substrates such as SiC or GaN for future mass production.[11] This progress ensures that β-Ga_2O_3 can potentially meet or exceed the performance of Si and typical wide bandgap semiconductors such as SiC or GaN for ultrahigh-voltage power switching devices.[12]

Recently, β-Ga_2O_3 epilayers have been grown on different substrates by various growth techniques, such as Metal-Organic Chemical Vapor Deposition (MOCVD), Molecular Beam Epitaxy (MBE), and Pulsed Laser Deposition (PLD). These advanced growth techniques offer versatile heterostructures with precise control over the interface. Sapphire (α-Al_2O_3) is generally used as a low-cost substrate. In contrast to the poor lattice match between sapphire and GaN (∼13.8%),[13] the lattice mismatch between β-Ga_2O_3 and sapphire is significantly lower. The mismatch in spacing between the oxygen atoms in the (−201) equivalent plane of β-Ga_2O_3 is about 6.6% for the *c*-plane sapphire.[14] The lattice mismatch between β-Ga_2O_3 and GaN is found to be smaller. The in-plane lattice mismatch between the (−201) plane of β-Ga_2O_3 and the (0002) plane of GaN is as low as 4.7%;[15] thus, it could be used for high quality β-Ga_2O_3 growth. So far, sapphire, GaN/sapphire template, and β-Ga_2O_3 native substrate are the most commonly studied substrates for the growth of β-Ga_2O_3 epilayers. However, the epilayers suffer from the relatively large lattice mismatch except when using the native substrates which are too costly.[16–18] Thus, substrates with a lower lattice mismatch with the (−201) plane of β-Ga_2O_3 are needed to facilitate the integration of β-Ga_2O_3 with nitrides in the formation of heterostructures for device applications.

Furthermore, band offset is one of the most important electronic parameters in the design of the β-Ga_2O_3-based semiconductor heterojunction because it determines the energy barriers for electron and hole transport, essential for the operation of electronic and optical devices. In the literature, few studies show measurements of the band offset of β-Ga_2O_3 with other semiconductor heterojunctions by X-ray photoemission spectroscopy (XPS). Chen *et al.* reported the band alignment of β-Ga_2O_3/Si heterojunctions grown by PLD and found that the valence band offset (VBO) was 3.5 eV.[19] On the other hand, the band offsets of the β-Ga_2O_3/GaN and β-Ga_2O_3/6H-SiC were found to be 1.4 eV[20] and 2.8 eV,[21] respectively. Furthermore, the band discontinuities between β-Ga_2O_3/Al_2O_3 and β-Ga_2O_3/$LaAl_2O_3$ were also identified.[22,23]

In this paper, we report the growth of β-Ga_2O_3 on the AlN/sapphire template by PLD to form a β-Ga_2O_3/AlN heterojunction. First of all, the lattice mismatch between the (−201) plane of β-Ga_2O_3 and the (0002) plane of AlN is elaborated. We find that their lattice mismatch is much smaller by

comparing with the (−201) β-Ga_2O_3 grown on a (0002) GaN template. Then, the determination of the valence and conduction band offsets (VBO and CBO) is presented and the type of heterojunction is identified.

Figure 1(a) schematically shows the atomic-arrangement model for the interface between the (−201) β-Ga_2O_3 on top of (0002) AlN and its epitaxial relationship (from the cross-sectional point of view). The projection is along the *b*-axis of β-Ga_2O_3 and the [11-20] direction of AlN. In AlN, Al atoms are present on the surface. The (−201) plane of β-Ga_2O_3 is parallel with the (0002) plane of AlN and the [102] direction of β-Ga_2O_3 with the [-1100] direction of AlN. The O atoms in the β-Ga_2O_3 are bonded with Ga atoms at the interface, as shown in Fig. 1(a). Figure 1(b) shows the top view of the atomic-arrangement of both β-Ga_2O_3 and AlN. The Ga and O atoms in β-Ga_2O_3 and the Al and N atoms in AlN are both arranged in a hexagonal pattern but with slightly different sizes of hexagons. In each hexagon, there are three cations and three anions. Based on the lattice constants of β-Ga_2O_3 and AlN, the side length (marked as "*l*" in the figure) of the hexagon in β-Ga_2O_3 is 1.753 Å and that of AlN is 1.797 Å, which determined that the lattice mismatch between (−201) β-Ga_2O_3 along the *b*-axis and (0002) AlN is around 2.4%. This value is much smaller than the lattice mismatch between (−201) β-Ga_2O_3 on (0002) GaN and (−201) β-Ga_2O_3 on sapphire which are 4.7%[15] and 6.6%,[14] respectively. Thus, (0002) AlN could be a better template for the (−201) β-Ga_2O_3 epilayer growth and vice versa.

The AlN/sapphire templates were grown by MOCVD, and the details of the AlN template growth have been reported in our previous articles. Prior to the deposition, the AlN/sapphire templates were cleaned ultrasonically with acetone (10 min) followed by isopropyl alcohol (5 min) and then rinsed with deionized water. The β-Ga_2O_3 layers on the AlN/sapphire templates were grown by a Neocera Pioneer 180 PLD using a 1 in. β-Ga_2O_3 ceramic target (99.99% purity). A KrF excimer laser ($\lambda = 248$ nm) was used to ablate the target at a pulse frequency of 5 Hz and an energy per pulse of ∼400 mJ. The distance between the target and the substrate was fixed at 5 cm. After the chamber was pumped down to a base pressure of 5×10^{-8} mbar, the substrate was gradually heated to 625 °C. Oxygen gas was introduced into the chamber to achieve a stable working pressure of 50 mbar during the deposition process. In the deposition, 15 000 and 390 pulses were used to achieve thicknesses of ∼140 and ∼1.5 nm for the β-Ga_2O_3 layers, respectively. To determine the band offsets at the β-Ga_2O_3/AlN heterointerface, three samples were investigated: thick (∼140 nm) β-Ga_2O_3 on the AlN/sapphire template (sample A), AlN/sapphire template (sample B), and thin (∼1.5 nm) β-Ga_2O_3 on the AlN/sapphire template (sample C).

The structural properties of these samples were examined by using a Bruker D8 Advance X-ray diffractometer (XRD) using Cu Kα ($\lambda = 1.5405$ Å) radiation and a Horiba Aramis Micro-Raman system with a backscattering geometry. The samples were excited using a 325 nm He-Cd laser, and the Raman signal was collected using a monochromator equipped with a 2400 lines/mm grating.

From the XRD pattern of sample A, as shown in Fig. 2(a), we notice that besides the substrate diffraction peaks at 36.1° and 41.1° from (0002) AlN and *c*-plane sapphire substrate, there are three other peaks at 18.9°, 38.3°, and 59.1° which corresponds to (−201), (−402), and (−603) planes of β-Ga_2O_3, respectively.[24] Figure 2(b) displays the micro-Raman spectra, confirming the β-Ga_2O_3 layer on AlN/sapphire by observing the Raman peaks at 168 and 201 cm^{-1} where the phonon modes are in good agreement with the previous report.[25] These two peaks are not observed in sample C due to the extreme thin β-Ga_2O_3 layer (∼1.5 nm). Raman peaks originating from the AlN and sapphire substrate are also displayed.[26]

Furthermore, high-angle annular dark field scanning transmission electron microscopy (HAADF-STEM) was applied to investigate sample C by operating a probe corrected FEI Titan at an acceleration voltage of 300 kV. The TEM specimens were prepared by using FEI's Helios dual beam focused ion beam (FIB)/SEM equipped with an Omniprobe. Energy-dispersive X-ray spectroscopy (EDX) acquisition was performed to detect the elemental distribution at the interface. Figure 3(a) shows the cross-sectional STEM image of the interface between the β-Ga_2O_3 and AlN layers. Figure 3(b) presents the elemental distribution from the EDX scan of Ir, N, Al, Ga, and O across the interface, confirming a uniform distribution of the elements in the grown layer. Ir was sputtered on the surface to act as a conductive layer to prevent severe surface charging during the TEM sample preparation. An extremely thin layer (∼1.5 nm) of β-Ga_2O_3 was observed based on the Ga mapping result. Due to the monoclinic structure of β-Ga_2O_3 with lattice parameters a = 12.23 Å, b = 3.04 Å, c = 5.80 Å, and $\beta = 103.7°$ (the angle between "a" and "c" axes),[27] we may only have a total of 2–3 unit cells of β-Ga_2O_3 in the grown layer vertically. The significant presence of O atoms in the deposited Ir layer indicated the formation of IrO_2. Due to the extreme thin β-Ga_2O_3 layer (∼1.5 nm), it was difficult to measure its crystallinity.

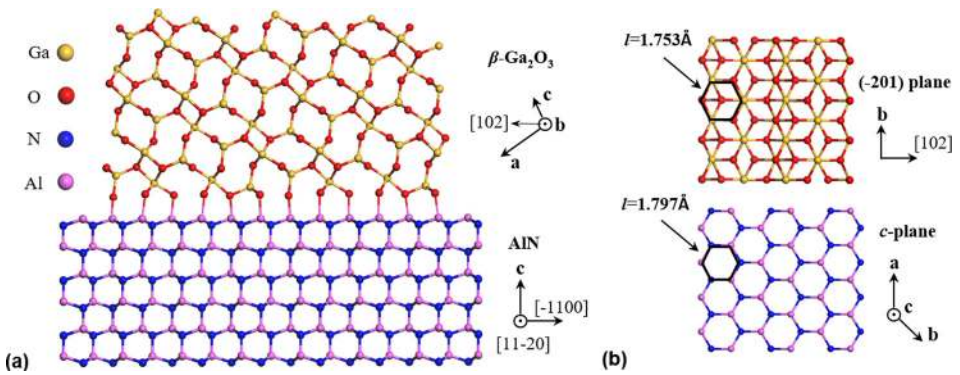

FIG. 1. (a) Atomic arrangement model of the interface between (−201) β-Ga_2O_3 and (0002) AlN. (b) The hexagonal pattern of the atomic arrangement in both the (−201) plane of β-Ga_2O_3 and (0002) plane of AlN.

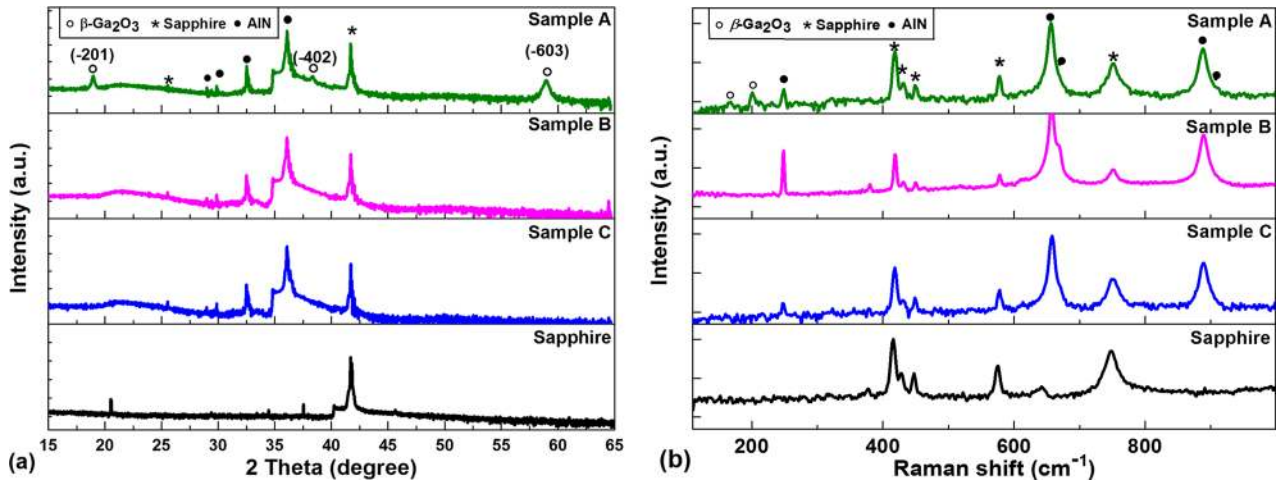

FIG. 2. (a) XRD 2θ-ω scan of on-axis reflections of samples A, B, and C and sapphire substrate. (b) Micro-Raman spectra of samples A, B, and C and sapphire substrate.

However, we have confirmed the single crystallinity of the β-Ga_2O_3 layer under the same growth condition in a thick β-Ga_2O_3 layer by comparing its epitaxial relationship with the substrates, similar to earlier reports in which the single-crystal β-Ga_2O_3 layers were also obtained by using the same growth technique.[28,29]

Lastly, the band offset measurement for this heterojunction was performed. All core levels (CLs) and valence band photoemission spectra of the β-Ga_2O_3 and AlN/sapphire substrate were measured by using a high-resolution XPS (HR-XPS) method. The HR-XPS measurements were carried out using a Kratos Axis Ultra DLD spectrometer equipped with a monochromatic Al Kα X-ray source ($h\nu = 1486.6$ eV) operating at 150 W, a multi-channel plate, and a delay line detector under a vacuum of $\sim 10^{-9}$ mbar. The binding energy of the C 1s peak (284.8 eV) was used as a standard reference. The details of the XPS setup have been described in previous studies on different heterojunctions.[30,31] To evaluate the VBO at the β-Ga_2O_3/AlN interface, we need to determine the energy difference between the Ga and Al CLs from sample C and also the energy of CLs relative to the respective VBMs of samples A and B. Also, the CLs of Ga 3d and Al 2p were chosen in the analysis. From the theory first introduced by Kraut, for the β-Ga_2O_3/wurtzite AlN heterojunction, the VBO (ΔE_v) can be calculated from the following formula:[32]

$$\Delta E_v = \left(E^{Ga2O3}_{Ga\,3d} - E^{Ga2O3}_{VBM}\right) - \left(E^{AlN}_{Al\,2p} - E^{AlN}_{VBM}\right) + \left(E^{Ga2O3}_{Ga\,3d} - E^{AlN}_{Al\,2p}\right). \quad (1)$$

The first term on the right side of the equation is the CL energy of Ga 3d determined with respect to the VBM of sample A.

Figure 4(a) shows the Ga 3d CL spectrum collected from the β-Ga_2O_3 layer which indicates a single peak at 20.33 eV, corresponding to the Ga-O bond. Figure 4(b) depicts the valence band spectrum where the VBM of the sample is obtained by linearly extrapolating the leading edge to the baseline of the respective valence band photoelectron spectrum. The VBM of the β-Ga_2O_3 is measured to be 3.35 eV. Thereby, the separation between the CL energies of Ga 3d and VBM $[\Delta E = (E^{Ga2O3}_{Ga\,3d} - E^{Ga2O3}_{VBM})]$ for β-Ga_2O_3 is 16.98 eV, which is in accordance with the results reported by Chang *et al.*[21]

To calculate the term in the second bracket in Eq. (1), the XPS spectrum of sample B was collected. We observe that the CL of Al 2p is located at 73.08 eV from the AlN layer [Fig. 5(a)], while the VBM is measured to be 2.4 eV [Fig. 5(b)]. Thereby, the separation between the CL energy of Al 2p and the VBM $[\Delta E = (E^{AlN}_{Al\,2p} - E^{AlN}_{VBM})]$ for the AlN layer is determined to be 70.68 eV. The last term in Eq. (1) represents the CL separation between the Ga 3d and Al 2p peaks that was measured from the XPS spectrum of sample C. Figures 6(a) and 6(b) show the Ga 3d and Al 2p CLs which originated from sample C, respectively. Figure 6(a) demonstrates a single peak in the Ga 3d CL spectrum, showing the Ga 3d chemical state at 20.45 eV. The Al 2p CL is located at 73.60 eV [Fig. 6(b)]. The energy difference between the CLs of Ga 3d and Al 2p $[\Delta E = (E^{Ga2O3}_{Ga\,3d} - E^{AlN}_{Al\,2p})]$ is -53.15 eV. Thus, the

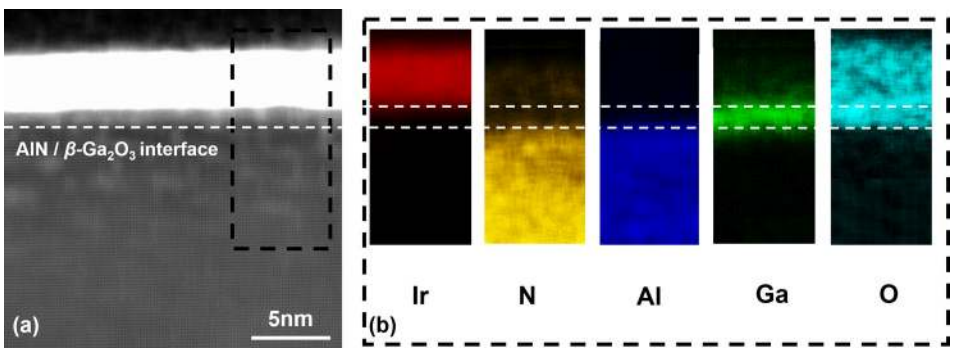

FIG. 3. (a) Cross-sectional HAADF-STEM [11-20] image of sample C at the heterojunction interface. (b) The EDX elemental map of Iridium (Ir), N, Al, Ga, and O from the white dashed area in (a). The white dashed line marks the interface of β-Ga_2O_3/AlN and β-Ga_2O_3 with the Ir layer.

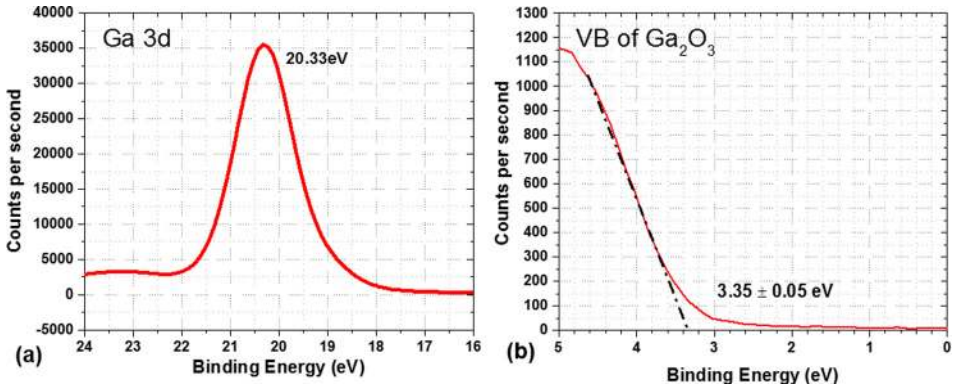

FIG. 4. (a) The CL of Ga 3d and (b) the valence band spectra of the β-Ga_2O_3 layer (sample A).

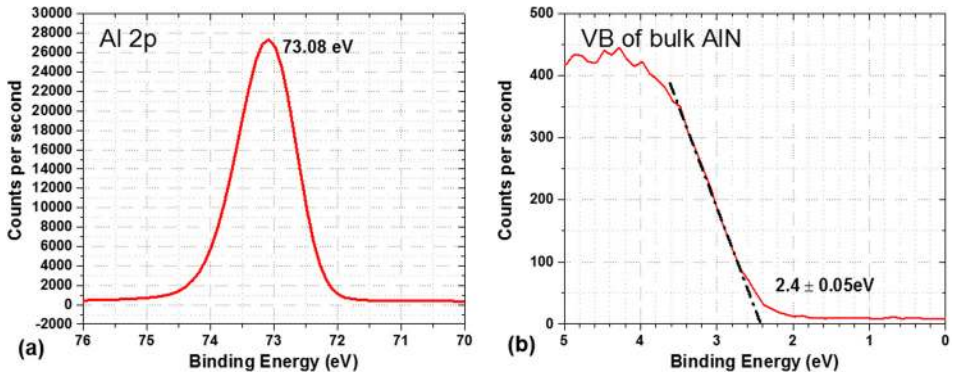

FIG. 5. (a) The CL of Al 2p and (b) the valence band spectra of the AlN layer (sample B).

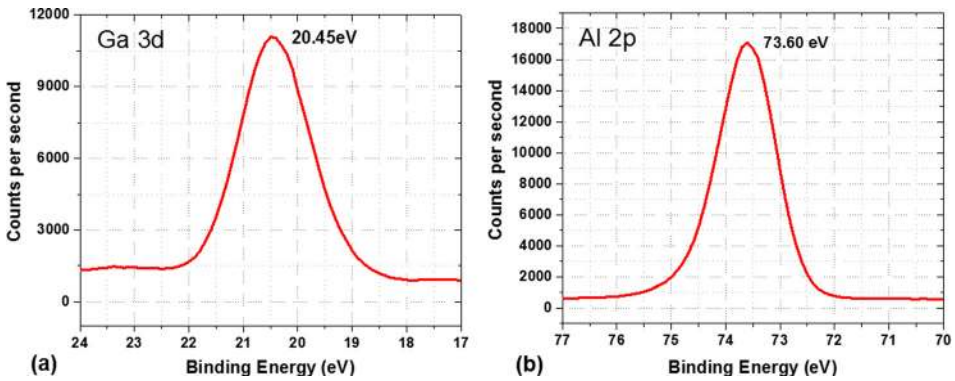

FIG. 6. (a) The CLs of Ga 3d and (b) the Al 2p spectra of the β-Ga_2O_3/AlN heterojunction (sample C).

VBO can be determined to be $\Delta Ev = -0.55 \pm 0.05$ eV using Eq. (1).

Thereby, by substituting the VBO (ΔE_v) and the electronic bandgap values of β-Ga_2O_3 ($E_g = 4.9$ eV)[33] and AlN ($E_g = 6.1$ eV)[1] in Eq. (2), we can measure the CBO (ΔE_c) for the β-Ga_2O_3/AlN heterostructure

$$\Delta E_c = \left(E_g^{Ga2O3} + \Delta E_v - E_g^{AlN}\right). \quad (2)$$

Hence, based on Eq. (2), the resultant CBO (i.e., ΔE_c) is -1.75 ± 0.05 eV. Inevitably, there was tensile strain in the β-Ga_2O_3 epilayer due to the heteroepitaxial growth. However, studies have shown that the effect of strain on both CBO and VBO was almost negligible by comparing the strained and unstrain heterojunctions, generally less than 0.1 eV.[34,35] Furthermore, considering the fact that the bandgap values of β-Ga_2O_3 thin film range widely between 4.5 and 4.9 eV grown by different techniques and conditions,[33,36,37] we must calibrate its bandgap value and the band offset values under specific growth conditions while designing the β-Ga_2O_3-containing heterojunction for device application.

The experimentally determined parameters from this study are incorporated into a band alignment diagram as shown in Fig. 7. This figure suggests that the β-Ga_2O_3/AlN heterostructure is a type-II heterostructure. This unique bandgap alignment between β-Ga_2O_3/AlN could aid the development of power devices. By using the band alignment of GaN and AlN at room temperature reported by Van de Walle and Neugebauer,[1] we also plot the band alignment of β-Ga_2O_3/AlN along with GaN in Fig. 7. The VBO of AlN/GaN is 1.12 eV.[38] Based on the diagram, we obtain the VBO and CBO of the β-Ga_2O_3/GaN heterojunction of 1.35 and 0.15 eV, respectively. These results are in good agreement with the experimental results of band offset parameters reported earlier by Wei *et al.* in which they showed that the VBO and CBO of β-Ga_2O_3/GaN are 1.40 and 0.10 eV, and also a type-I heterojunction can be formed in the β-Ga_2O_3/GaN heterojunction. These characteristics could offer numerous

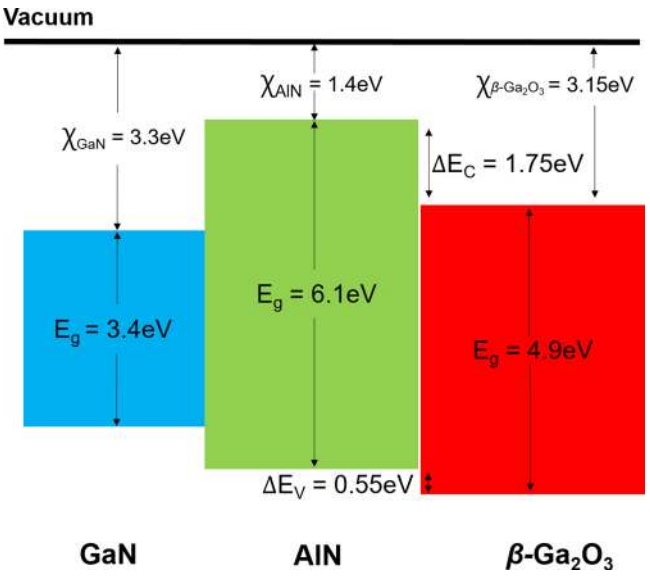

FIG. 7. The band alignment diagram of the β-Ga_2O_3/AlN heterojunction, along with that of GaN.

degrees of freedom and provide further guidance for designing power devices by using a combination of β-Ga_2O_3 with conventional III-nitrides. For example, the $Al_xGa_{1-x}N/\beta$-Ga_2O_3 $(0 \leq x \leq 1)$-based heterojunction can be designed and grown. With the addition of Ga in AlN, the CBO would gradually reduce, easing the electron transport and eventually reach zero at the Ga composition of around 92% assuming the Vegard's law with no bowing. With the higher composition of Ga in $Al_xGa_{1-x}N$, the heterojunction finally turns into the type-I heterojunction as mentioned above. Thus, the $Al_xGa_{1-x}N/\beta$-Ga_2O_3 heterojunction can be potentially employed for ultraviolet (UV) detectors or light emitting diodes because the β-Ga_2O_3 is a transparent material in the UV region due to the fact that it has a wide bandgap and high-quality n-type Ga_2O_3 bulk crystals are commercially available.

In summary, we have deposited β-Ga_2O_3 layers by PLD on the MOCVD-grown AlN/sapphire templates to form a heterojunction. The lattice mismatch between β-Ga_2O_3 and wurtzite AlN is only 2.4% which is the smallest value compared to other binary nitride materials such as GaN, BN, and InN. The determination of the band offset parameters at the β-Ga_2O_3/AlN heterostructure was carried out by using the HR-XPS. We determined the VBO and CBO to be -0.55 eV and -1.75 eV, respectively, with a type-II heterostructure band alignment. We also plotted the band alignment of the β-Ga_2O_3/AlN heterojunction along with the GaN which could provide valuable support in the design of β-Ga_2O_3-based heterostructures for future device applications.

The KAUST authors would like to acknowledge the support of Baseline BAS/1/1664-01-01 and Professor Russell D. Dupuis from the Georgia Institute of Technology for supplying the AlN/sapphire template.

[1]C. G. Van de Walle and J. Neugebauer, Nature **423**, 626 (2003).
[2]B. Janjua, H. Sun, C. Zhao, D. H. Anjum, D. Priante, A. A. Alhamoud, F. Wu, X. Li, A. M. Albadri, A. Y. Alyamani, M. M. El-Desouki, T. K. Ng, and B. S. Ooi, Opt. Express **25**, 1381 (2017).
[3]T. D. Moustakas and R. Paiella, Rep. Prog. Phys. **80**, 106501 (2017).
[4]N. Alfaraj, S. Mitra, F. Wu, I. Ajia, B. Janjua, A. Prabaswara, R. A. Aljefri, H. Sun, T. K. Ng, B. S. Ooi, I. S. Roqan, and X. Li, Appl. Phys. Lett. **110**, 161110 (2017).
[5]M. Higashiwaki, K. Sasaki, A. Kuramata, T. Masui, and S. Yamakoshi, Appl. Phys. Lett. **100**, 013504 (2012).
[6]M. A. Mastro, A. Kuramata, J. Calkins, J. Kim, F. Ren, and S. J. Pearton, ECS J. Solid State Sci. Technol. **6**, P356 (2017).
[7]K. Konishi, K. Goto, H. Murakami, Y. Kumagai, A. Kuramata, S. Yamakoshi, and M. Higashiwaki, Appl. Phys. Lett. **110**, 103506 (2017).
[8]J. Kim, S. Oh, M. Mastro, and J. Kim, Phys. Chem. Chem. Phys. **18**, 15760 (2016).
[9]A. M. Armstrong, M. H. Crawford, A. Jayawardena, A. Ahyi, and S. Dhar, J. Appl. Phys. **119**, 103102 (2016).
[10]Z. Liu, T. Yamazaki, Y. Shen, T. Kikuta, N. Nakatani, and Y. Li, Sens. Actuators, B **129**, 666 (2008).
[11]A. Kuramata, K. Koshi, S. Watanabe, Y. Yamaoka, T. Masui, and S. Yamakoshi, Jpn. J. Appl. Phys., Part 1 **55**, 1202A2 (2016).
[12]M. Higashiwaki, K. Sasaki, A. Kuramata, T. Masui, and S. Yamakoshi, Phys. Status Solidi A **211**, 21 (2014).
[13]R. C. Powell, N.-E. Lee, Y.-W. Kim, and J. E. Greene, J. Appl. Phys. **73**, 189 (1993).
[14]S. Nakagomi and Y. Kokubun, J. Cryst. Growth **349**, 12 (2012).
[15]M. M. Muhammed, M. Peres, Y. Yamashita, Y. Morishima, S. Sato, N. Franco, K. Lorenz, A. Kuramata, and I. S. Roqan, Appl. Phys. Lett. **105**, 042112 (2014).
[16]M. J. Tadjer, M. A. Mastro, N. A. Mahadik, M. Currie, V. D. Wheeler, J. A. Freitas, Jr., J. D. Greenlee, J. K. Hite, K. D. Hobart, C. R. Eddy, Jr., and F. J. Kub, J. Electron. Mater. **45**, 2031 (2016).
[17]T. Oshima, T. Okuno, and S. Fujita, Jpn. J. Appl. Phys., Part 1 **46**, 7217 (2007).
[18]A. J. Green, K. D. Chabak, E. R. Heller, R. C. Fitch, M. Baldini, A. Fiedler, K. Irmscher, G. Wagner, Z. Galazka, S. E. Tetlak, A. Crespo, K. Leedy, and G. H. Jessen, IEEE Electron Device Lett. **37**(7), 902 (2016).
[19]Z. W. Chen, K. Nishihagi, X. Wang, K. Saito, T. Tanaka, M. Nishio, M. Arita, and Q. X. Guo, Appl. Phys. Lett. **109**, 102106 (2016).
[20]W. Wei, Z. Qin, S. Fan, Z. Li, K. Shi, Q. Zhu, and G. Zhang, Nanoscale Res. Lett. **7**, 562 (2012).
[21]S. H. Chang, Z. Z. Chen, W. Huang, X. C. Liu, B. Y. Chen, Z. Z. Li, and E. W. Shi, Chin. Phys. B **20**, 116101 (2011).
[22]P. H. Carey, F. Ren, D. C. Hays, B. P. Gila, S. J. Pearton, S. Jang, and A. Kuramata, Vacuum **142**, 52 (2017).
[23]P. H. Carey, F. Ren, D. C. Hays, B. P. Gila, S. J. Pearton, S. Jang, and A. Kuramata, J. Vac. Sci. Technol., B **35**, 041201 (2017).
[24]K. D. Leedy, K. D. Chabak, V. Vasilyev, D. C. Look, J. J. Boeckl, J. L. Brown, S. E. Tetlak, A. J. Green, N. A. Moser, A. Crespo, D. B. Thomson, R. C. Fitch, J. P. McCandless, and G. H. Jessen, Appl. Phys. Lett. **111**, 012103 (2017).
[25]C. Kranert, C. Sturm, R. Schmidt-Grund, and M. Grundmann, Sci. Rep. **6**, 35964 (2016).
[26]M. Kubal, Surf. Interface Anal. **31**, 987 (2001).
[27]J. Åhman, G. Svensson, and J. Albertsson, Acta Crystallogr., Sect. C: Cryst. Struct. Commun. **52**, 1336 (1996).
[28]F.-P. Yu, S.-L. Ou, and D.-S. Wuu, Opt. Mater. Express **5**, 1240 (2015).
[29]L. M. Garten, A. Zakutayev, J. D. Perkins, B. P. Gorman, P. F. Ndione, and D. S. Ginley, MRS Commun. **6**, 348 (2016).
[30]H. Sun, Y. Park, K.-H. Li, C. T. Castanedo, A. Alowayed, T. Detchprohm, R. Dupuis, and X. Li, Appl. Phys. Lett. **111**, 122106 (2017).
[31]M. Tangi, P. Mishra, C. Tseng, T. K. Ng, M. N. Hedhili, D. H. Anjum, M. S. Alias, N. Wei, L. Li, and B. S. Ooi, ACS Appl. Mater. Interfaces **9**, 9110 (2017).
[32]E. A. Kraut, R. W. Grant, J. R. Waldrop, and S. P. Kowalczyk, Phys. Rev. Lett. **44**, 1620 (1980).
[33]A. Segura, L. Artús, R. Cuscó, R. Goldhahn, and M. Feneberg, Phys. Rev. Mater. **1**, 024604 (2017).
[34]C. G. Van de Walle and J. Neugebauer, Appl. Phys. Lett. **70**, 2577 (1997).
[35]S. Wei and A. Zunger, Appl. Phys. Lett. **69**, 2719 (1996).
[36]S. Rafique, L. Han, S. Mou, and H. Zhao, Opt. Mater. Express **7**, 3561 (2017).
[37]S. I. Stepanov, V. I. Nikolaev, V. E. Bougrov, and A. E. Romanov, Rev. Adv. Mater. Sci. **44**, 63 (2016), available at http://www.ipme.ru/e-journals/RAMS/no_14416/06_14416_stepanov.pdf.
[38]S. Vitanov, "Simulation of high electron mobility transistors," Ph.D. dissertation, Technischen Universität Wien, 2010.